Optica Applicata, Vol. LIII, No. 2, 2023
DOI: 10.37190/oa230205

Research on peripheral clamping of large-aperture laser transport mirror

TingFen Cao[1], Bowu Liu[2,*], Hui Wang[2], Wei Ni[1], Jinli Zhang[1], Xiaojuan Chen[3], YinGang Li[1], Hai Zhou[1], Xiaodong Jiang[1], Dongxia Hu[1], Qihua Zhu[1]

[1]China Academy of Engineering Physics, Research Center of Laser Fusion, Youxian District, Mianyang, China, 621900

[2]Tsinghua University, Department of Mechanical Engineering, Haidian District, Beijing, China, 100084

[3]China Academy of Engineering Physics, Institute of Systems Engineering, Youxian District, Mianyang, China, 621900

*Corresponding author: lbw20@mails.tsinghua.edu.cn

This article introduces the study of peripheral clamping for large-aperture laser mirrors in high power laser facilities. Some multi-point clamping schemes were experimentally tested, the results of the experiments show that these schemes cannot meet the technical requirements, and in the simulation analysis, we explain the reason for this phenomenon. It is concluded that the additional bending moment caused by the non-ideal process factors in the multi-point clamping is the main cause for the surface distortion. Based on the above conclusions, we carried out research on minor-point clamping. Experimental verification of the minor-point clamping were done, the results show that the minor-point clamping can meet the requirements of technical indicators in whole process. This work can provide a reference for the design of the large-aperture transport mirror clamping structure, which may be used in huge laser devices and telescopes.

Keywords: transport mirror, peripheral clamping, surface distortion, assembly structure.

1. Introduction

The large-aperture laser transport mirror is an important part of the high-power laser system. Its function is to spatially group and project the fundamental frequency laser output from the main amplification system according to a certain beaming method, so that the main laser can incident into the final optics assembly according to the designed path [1]. Generally, according to physical experiment requirements for beam arrangement and grouping, a beam group in a high-power laser system needs to be designed with 4–6 transmission mirrors to realize laser grouping and transmission [2].

The surface distortion of the transport mirror directly affects the wavefront of the main laser beam, thereby deteriorating the quality of the focal spot, so it needs to be

controlled [3–5]. The surface accuracy of the large-aperture mirror is mainly determined by processing and assembly. At the current level of manufacturing technology, the surface PV of the large-aperture laser transport mirror can be controlled below 150 nm after ultra-precision grinding and polishing [6]. To further improve the surface accuracy, the manufacturing cost will be greatly increased, so it is important to reduce the additional surface distortion caused by clamping. According to the design of the high-power laser system, take the National Ignition Facility as an example [7], the additional surface distortion caused by assembly is required to be less than 0.25λ, where $\lambda = 632.8$ nm.

At present, the clamping methods of large-aperture mirrors mainly include back support [8] and peripheral clamping [9]. The peripheral clamping is to clamp the four sides of the mirror by using dozens of rubber nails, so that the single clamping force on the mirror will be dispersed. However, as the number of rubber nails increases, the geometric error of the nails, friction factor, lubrication conditions, tightening speed and other factors will make it difficult to control the pre-tightening force of the nails accurately, and it may cause the distortion of the mirror surface to be out of tolerance [10, 11].

In this paper, we carried out simulation calculations for peripheral clamping, analyzed the influence of different clamping schemes on the distortion of the mirror surface, and conducted a series of clamping experiments on the large-aperture laser transport mirror by using the originally designed assembly structure. Based on the conclusions obtained from the experiments and simulations, we optimized the clamping scheme and verified it by experiments, the results indicate that the minor-point clamping meets the technical requirement.

2. Peripheral clamping for large-aperture laser mirrors

The peripheral clamping structure for the large-aperture transport mirrors of the high-power laser system is shown in Fig. 1(a). The frame is the main load-bearing component, its dimensions are $670 \times 500 \times 90$ mm, and its thickness is 27 mm. The dimensions

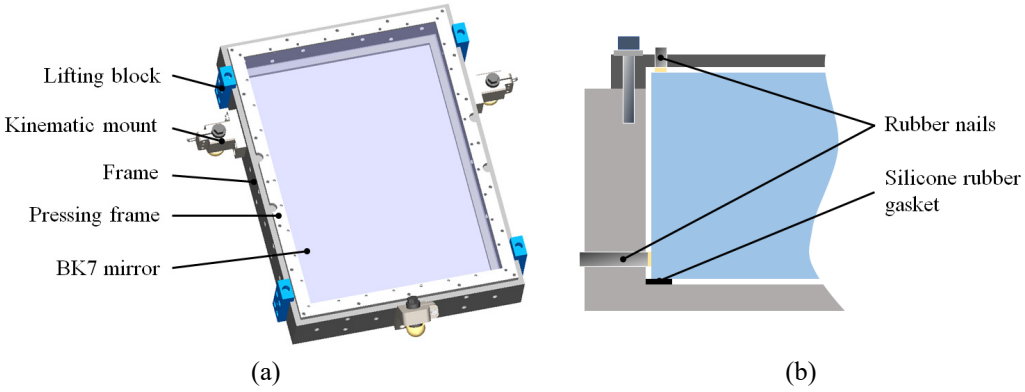

Fig. 1. (a) The peripheral clamping structure for the large-aperture transport mirrors. (b) The details of assembly structure which determine the distribution of clamping force on the mirror.

of the mirror are 610×440×85 mm. There are three rows of M6 threaded holes on the sides of the frame, and a row of M6 threaded holes on the pressing frame, which are used to install rubber nails. The details of the assembly structure are shown Fig. 1(b), the clamping force is provided by the rubber nails installed on the sides of the frame and the pressing frame, and there is a silicone rubber gasket at the bottom of the frame. The material bonded on the top of the rubber nails is PTFE, whose diameter and thickness are 4.8 and 2 mm, respectively. The specific location and physical objects of rubber nails are shown in Fig. 2.

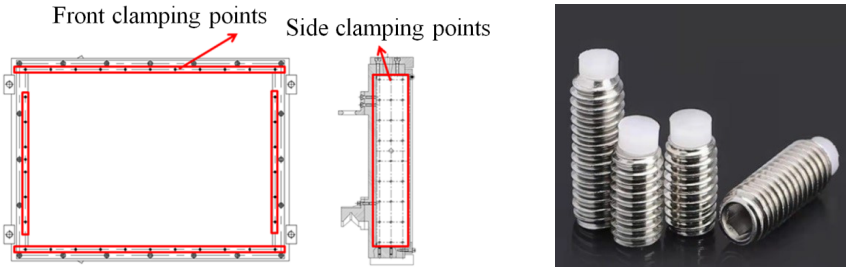

Fig. 2. (a) The specific location of rubber nails. (b) The physical objects of rubber nails.

The clamping scheme based on this assembly structure can be changed flexibly, so we can try a variety of clamping combinations, and perform experimental verification of these clamping schemes. In this way, we can filter out the clamping structure which can meet the engineering needs. Considering factors such as the stability of the structure, feasible peripheral clamping schemes are: full rubber nails on the front and full rubber nails on the sides; full rubber nails on the sides only; three-point rubber nails clamping on the front and full rubber nails on the sides; three-point rubber nails clamping on the front and two rubber nails on each side. All these clamping schemes were experimentally tested in our work.

3. Simulation analysis of the peripheral clamping

According to the assembly structure, the clamping force on the mirror can be divided into two categories: side clamping force and front clamping force. In the simulation analysis, we calculated the influence of the two types of clamping forces on the surface shape respectively, and the relevant regularities are as follows. The material of the mirror is BK7 glass, whose Young's modulus is 79.2 GPa, and Poisson ratio is 0.211. We modeled and simulated by using ANSYS Workbench.

In order to examine the influence of side clamping force alone, four clamping points were set on both opposite sides of the mirror. In the analysis, we mainly considered the influence of the value and position of the clamping force. Figures 3 and 4 show the simulation results for on-center and off-center clamping, respectively. In the simulation of off-center clamping, we offset the clamping point 25 mm from the centerline.

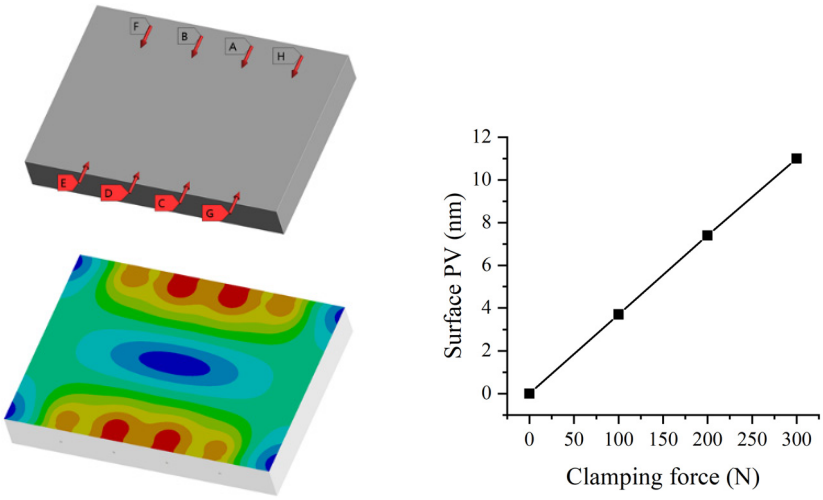

Fig. 3. Simulation results of centerline clamping on the sides. (a) Boundary load settings and typical surface distortion. (b) The relationship between the surface PV and the value of single clamping force.

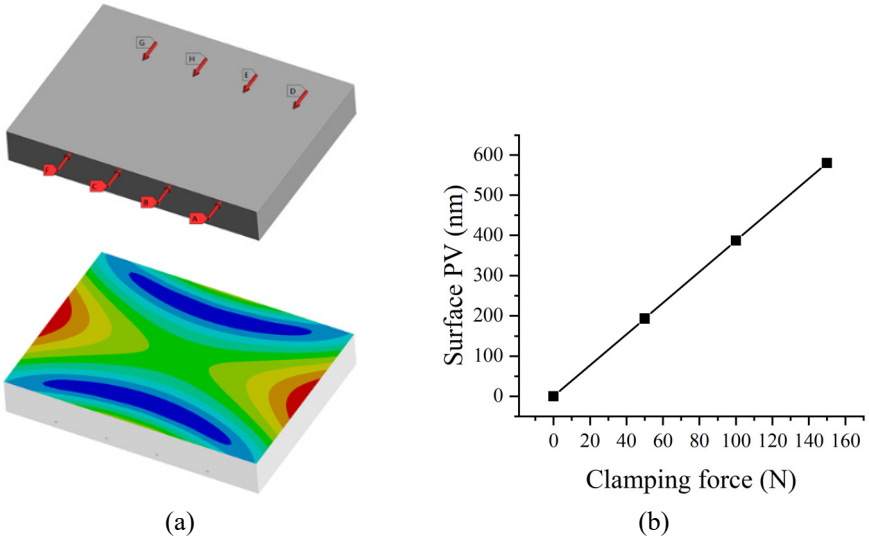

Fig. 4. Simulation results of off-center clamping on the sides. (a) Boundary load settings and typical surface distortion. (b) The relationship between the surface PV and the value of single clamping force.

As is shown in Fig. 3(b), when the total clamping force on the sides increases from 400 to 1200 N, the maximum surface PV is only 11 nm, which is almost negligible compared with the surface distortion caused by other factors. It means that when the side clamping forces applied to the centerline, it will not cause significant surface distortion. From the point of material mechanics, it is because that in this case there

is only normal stress in the mirror, so the surface distortion is only caused by Poisson effect.

As is shown in Fig. 4(b), when the total clamping force on the sides increases from 200 to 600 N, the surface PV increases from 193 to 580 nm, which is much higher than the surface distortion caused by centerline clamping. Compared with the centerline clamping, there is additional bending moment applied to the mirror in this case, which causes bending deformation of the mirror. So we can conclude that it is the bending moment caused by the non-ideal factor of side clamping who is the main cause of the surface distortion. In the assembly structure with three rows of clamping points on the sides, due to the positional deviation of the threaded holes and the difficulty of ensuring the same preload of each rubber nail, the additional bending moment will inevitably to be generated, resulting in surface distortion.

It can be speculated that if multi-point clamping is applied on the front, there will also be additional bending moment due to various non-ideal factors in practical applications, so we consider three-point frontal support which is the simplest statically indeterminate structure to avoid the influence of these non-ideal process factors to the greatest extent. We analyzed the influence of three-point front clamping on the surface distortion by simulation, and point-to-point clamping was used to avoid the uncertainty of the support point position caused by the uneven bottom surface.

As is shown in Fig. 5(a), there are significant surface distortions at the positions of the clamping points due to the concentrated loads applied on them, but the overall surface does not show obvious distortion, which is consistent with the Saint-Venant's principle. In actual use and experimental measurement, the clamping points are outside

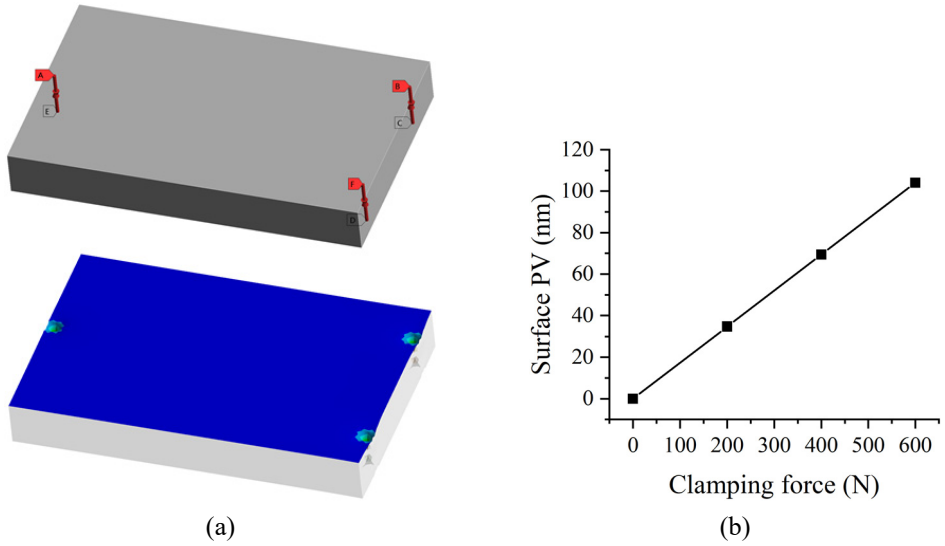

Fig. 5. Simulation results of three-point clamping on the front. (a) Boundary load settings and typical surface distortion. (b) The relationship between the surface PV in working aperture and the value of single clamping force.

the working aperture, so we removed the peripheral data, and calculated the distortion by using the surface shape data within the 570 ×400 mm working aperture only, and the results are shown in Fig. 5(b). The maximum surface PV is 104.1 nm, which meets the technical requirements, and the total support force in this case is 1800 N, which fully meets the requirements of structural stability.

Three-point clamping on the front and point-to-point clamping method can help to avoid the additional bending moment caused by over-restraint of multi-point clamping and uneven bottom surface effectively. The main difficulty is to ensure the collinearity of the corresponding clamping points, but compared with the process problems of multi-point clamping, it is easier to solve.

4. Experiments of multi-point clamping

4.1. Equipment and methods used in the experiments

The additional surface shape of the transport mirror caused by clamping is measured by a Φ600 near-infrared interferometer with an accuracy of 0.1λ, which is shown in Fig. 6(a). Considering the current measurement range of the interferometer, all the measurements were carried out in a vertical posture of the mirror, as is shown in Fig. 6(b). Firstly, we measured the surface shape of the mirror when there is bottom support only, and took this result as the initial surface shape of the mirror. Then we measured the surface shape of the mirror when it was clamped, and took the difference between the PV value of these two surface shapes as the additional surface shape. In order to further evaluate the performance of the clamping structure, in follow-up experiments, we added external excitation to the mirror, such as vibration and posture changes. The external excitation was mainly used to simulate the change from offline to online.

In order to ensure the consistency of the preload, we used a torque screwdriver to pre-tighten the rubber nails. The range of the torque screwdriver is 5–8 cN·m, and its accuracy is 5%.

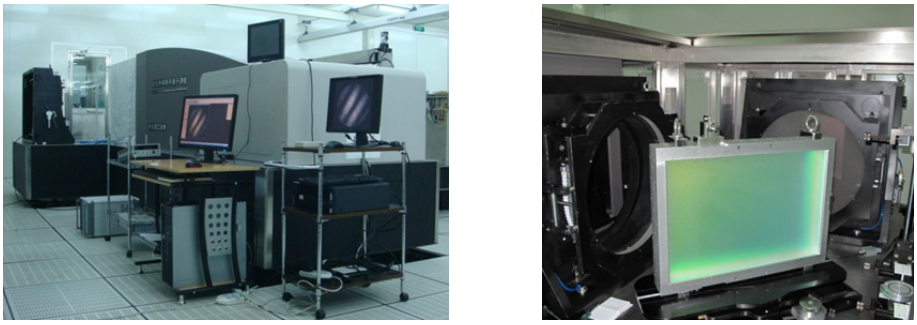

(a) (b)

Fig. 6. (a) Φ600 near-infrared interferometer. (b) Measuring posture of the mirror.

4.2. Experimental results of full rubber nails on the front and full rubber nails on the sides champing scheme

In this champing scheme, all the designed rubber nails were installed. During the experiment, we controlled the front tightening torque and the side tightening torque separately, where the front tightening torque decreased from 20 cN·m to 0 in steps of 5 cN·m, and the side tightening torque increased from 0 to 40 cN·m in steps of 20 cN·m. We set a return point every time the side tightening torque changed for one cycle, all the nails would be loosened to make the mirror return to the initial state. The typical clamping surface shape is shown in Fig. 7(a), it can be seen that the large-scale additional surface distortion caused by clamping is obvious, and results of surface PV are shown in Fig. 7(b).

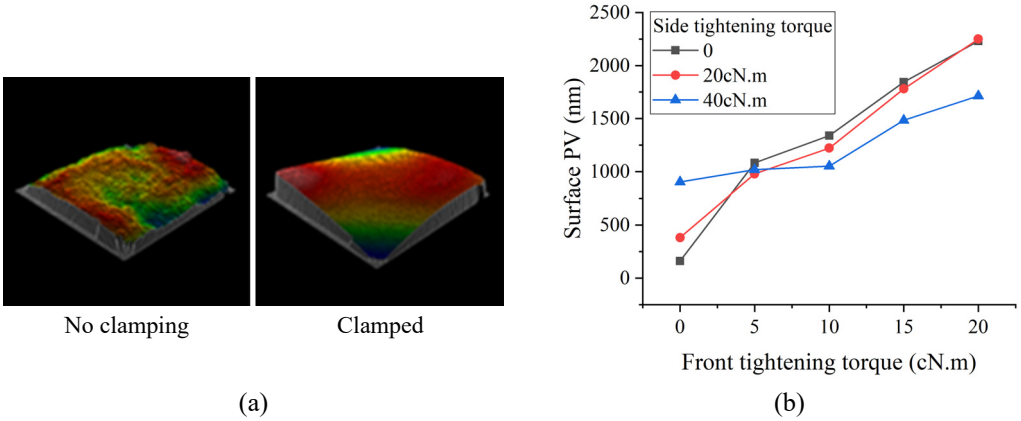

Fig. 7. Experimental results of full rubber nails on the front and full rubber nails on the sides champing scheme. (a) Typical clamping surface shape. (b) Results of surface PV.

As is shown in Fig. 7(b), when all the rubber nails are installed, the front tightening force has a more obvious influence on the surface distortion than the side tightening force, so the additional surface distortion decreases significantly as the front tightening force decreases. While when the front tightening force is the same, the additional surface distortion tends to decrease slightly as the side tightening force decreases, but when the front tightening force is small, this rule becomes invalid. The reason for this may be an accidental phenomenon that in this case the bending moments caused by the front clamping and the side clamping are exactly opposite.

Compared with the aforementioned technical requirements, it can be found that this scheme cannot meet the requirements. The reason for the obvious influence of the front clamping on the surface shape distortion is the uneven control of the clamping force, because it is difficult to ensure the positional accuracy of these so many threaded holes and the consistency of the preload on each point during manufacturing process. The non-uniform frontal pressure exerts additional moment on the flat, resulting in increased surface distortion.

4.3. Experimental results of full rubber nails on the sides only

Considering that the clamping on the front causes obvious additional distortion to the surface (which can be seen from the above experimental results), we conducted experiments on fixing the mirror by using the side clamping only. In order to improve the stability of the clamping, we added a copper sheet between the frame and the glass to improve the friction, which is shown in Fig. 8(a). In this experiment, we used a tightening force of 40 cN·m. This tightening force can meet the requirements of surface distortion and stability in the verification of the static clamping process.

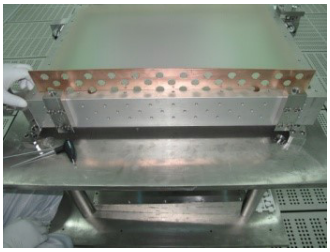

(a)

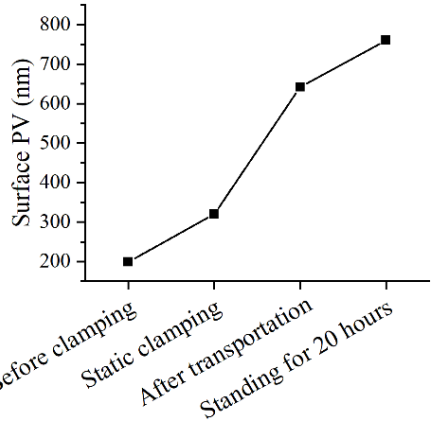

(b)

Fig. 8. Experimental results of full rubber nails on the sides only. (a) The experimental element with a copper sheet. (b) The change of surface PV in the whole process.

The results of the experiment are shown in Fig. 8(b). It can be seen that in the static state, the additional surface distortion meets the technical requirements. Therefore, we further investigated the performance of this scheme in the whole process, including transportation and standing for 20 hours after transportation. It can be seen that under external excitation, the additional surface distortion increased, and the final distortion exceeds the technical requirements. The instability of the structure which only the side clamping is used may be the main cause of the performance degradation.

4.4. Experimental results of three-point rubber nails clamping on the front and full rubber nails on the sides champing scheme

Since the stability of the structure is insufficient when only the sides are clamped, front clamping is still needed. According to the simulation analysis, we selected the three -point rubber nails clamping scheme on the front, which is the minimal number of statically determinate constraints. The full rubber nails clamping scheme was still applied on the sides, and the underside of the mirror was supported by a silicone rubber gasket.

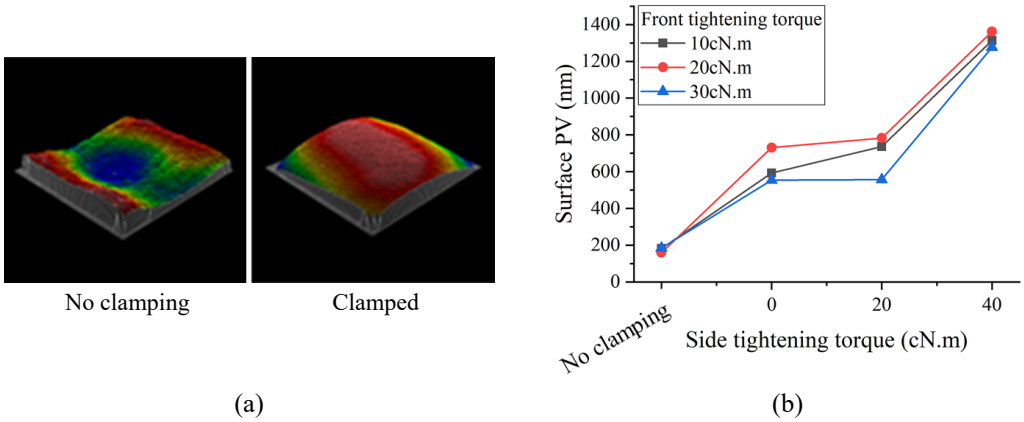

(a) (b)

Fig. 9. Experimental results of three-point rubber nails clamping on the front and full rubber nails on the sides champing scheme. (a) Typical clamping surface shape. (b) Results of surface PV.

The typical clamping surface shape is shown in Fig. 9(a), and the surface PV results are shown in Fig. 9(b).

As is shown in Fig. 9(b), when the side tightening force is the same, the change of the front tightening force has no obvious influence on the additional surface distortion. And compared with Fig. 7(b), when the value of the tightening force is the same, the additional distortion of the three-point clamping is smaller than the full rubber nails clamping scheme. This proves that the three-point clamping on the front helps to reduce additional surface distortion. However, compared with the technical requirements, it can be found that this scheme cannot meet the requirements too. According to the data in Fig. 9(b), when there is no side clamping, the front clamping results in part of the surface distortion, and with the increase of the side clamping force, the face shape distortion further increases. It means that in this case, the effect of three-point clamping on the front is reduced by non-ideal process factors because there is still multi-point clamping on the bottom surface of the mirror, which can cause harmful additional bending moments, while the multi-point clamping on the sides is actually difficult to avoid high additional surface distortion, although it used to perform well in the experiment of side clamping only.

5. Minor-point clamping

After the above experiments, we can see that none of the above peripheral clamping schemes can meet the technical requirements, so it is necessary to conduct further research on the clamping structure of the large-aperture laser transport mirror. Based on the conclusions of simulation analysis and multi-point clamping experiments, and referring to the mirror clamping structure of the French LMJ device [12], we carried out a series of experimental research on minor-point clamping.

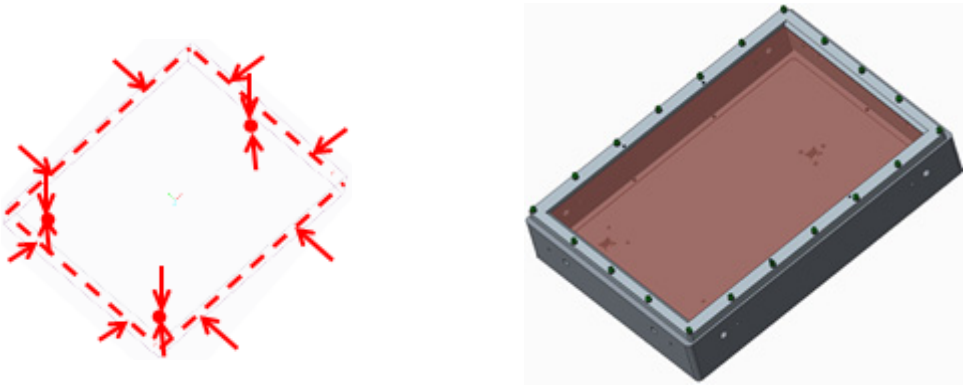

(a) (b)

Fig. 10. (a) Schematic diagram of the clamping force on the mirror. (b) Assembly model of minor-point clamping.

The schematic diagram of the minor-point clamping is shown in Fig. 10. Among them, the specification of the frame and the mirror are the same as the aforementioned. There are two threaded holes on each side of the frame which correspond to the centerline of the side of the mirror to minimize the additional bending moments due to non-uniformity of the side clamping force. And there are three threaded holes on the bottom of the frame for three-point clamping, at the same time, three bosses are set at the corresponding positions of the pressing plate to form a point-to-point clamping of the mirror with the rubber nails. In this way, the influence of non-uniformity of the front clamping force can be avoided.

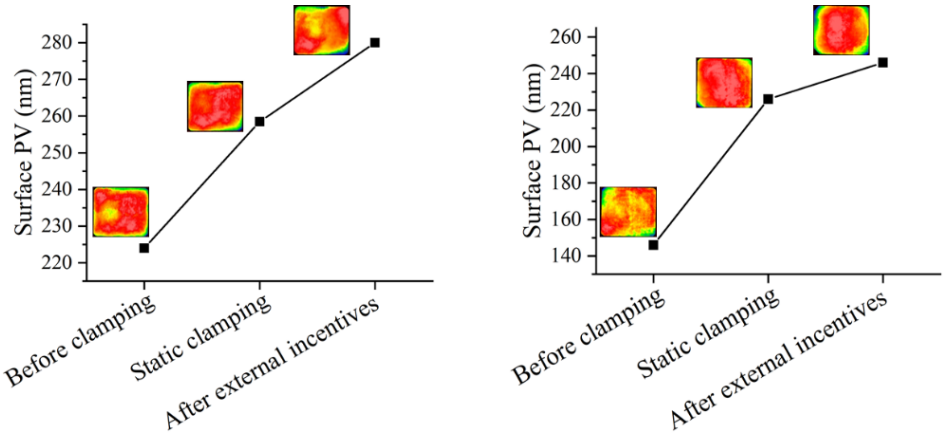

(a) (b)

Fig. 11. Experimental results of minor-point clamping. (a) Surface distortion of mirror #1. (b) Surface distortion of mirror #2.

We conducted experiments of minor-point clamping with two different mirrors as objects. In these experiments, we followed the equipment and methods used in the multi-point clamping experiments, and measured the mirror surface in the vertical state. For adequate support and stability, we set the front tightening torque and side tightening torque to 40 and 60 cN·m, respectively. In view of the experience gained from the experiments of side clamping only, we investigated the mirror surface of the whole process, the mirrors were transported after static clamping and then stood horizontally for up to 20 hours. The results are shown in Fig. 11.

Comparing the surface PV and technical requirements of surface distortion, it can be found that the minor-point clamping meets the requirements of related technical indicators in the whole process. It can also be seen from the measurement diagrams of the mirror surface that the distortion distribution of the mirror after clamping is still as random as before clamping, and there is no large-scale surface deformation similar to that in the multi-point clamping experiments. Therefore, the experimental results show that the minor-point clamping can fully meet the technical requirements.

6. Conclusion

In conclusion, this paper reports our researches on the peripheral clamping of large -aperture laser transmission mirrors in high power laser systems, clarifies the mechanism and laws of surface distortion caused by clamping, by simulation analysis and experiments, and finally verifies the qualification of the minor-point clamping in the whole process by experiments. In the simulation analysis, we investigated the influence of the side clamping and the front clamping on the surface distortion respectively. The results show that multi-row side clamping and multi-point front clamping are very susceptible to the non-ideal process factors, and then lead to additional bending moments, which is the main cause of surface distortion. The multi-point clamping experiment verifies the conclusions obtained from the simulation analysis and shows the necessity of front clamping for stability. Based on the above conclusions, we carried out research on minor-point clamping. The experimental results show that the minor -point clamping can meet the requirements of technical indicators in whole process (additional surface distortion caused by assembly is required to be less than 158 nm). This work can provide a reference for the design of the large-aperture transport mirror clamping structure, or other scenes that control the distortion of a large surface are needed.

Acknowledgments
This work was supported by National Natural Science Foundation of China (51975322), and Beijing Municipal Natural Science Foundation (3212006).

References

[1] Bonanno R.E., *Assembling and installing LRUs for NIF*, Proceedings of the SPIE, Vol. 5341, Optical Engineering at the Lawrence Livermore National Laboratory II: The National Ignition Facility, 2003: 137-145. https://doi.org/10.1117/12.538479

[2] Campbell J.H., Hawley-Fedder R.A., Stolz C.J., Menapace J.A., Borden M.R., Whitman P.K., Yu J., Runkel M.J., Riley M.O., Feit M.D., Hackel R.P., *NIF optical materials and fabrication technologies: an overview*, Proceedings of the SPIE, Vol. 5341, Optical Engineering at the Lawrence Livermore National Laboratory II: The National Ignition Facility, 2004: 102-119. https://doi.org/10.1117/12.538471

[3] Haynam C.A., Wegner P.J., Auerbach J.M., Bowers M.W., Dixit S.N., Erbert G.V., Heestand G.M., Henesian M.A., Hermann M.R., Jancaitis K.S., Manes K.R., Marshall C.D., Mehta N.C., Menapace J., Moses E., Murray J.R., Nostrand M.C., Orth C.D., Patterson R., Sacks R.A., Shaw M.J., Spaeth M., Sutton S.B., Williams W.H., Widmayer C.C., White R.K., Yang S.T., Van Wonterghem B.M., *National Ignition Facility laser performance status*, Applied Optics **46**(16), 2007: 3276-3303. https://doi.org/10.1364/AO.46.003276

[4] Spaeth M.L., Manes K.R., Kalantar D.H., Miller P.E., Heebner J.E., Bliss E.S., Spec D.R., Parham T.G., Whitman P.K., Wegner P.J., Baisden P.A., Menapace J.A., Bowers M.W., Cohen S.J., Suratwala T.I., Di Nicola J.M., Newton M.A., Adams J.J., Trenholme J.B., Finucane R.G., Bonanno R.E., Rardin D.C., Arnold P.A., Dixit S.N., Erbert G.V., Erlandson A.C., Fair J.E., Feigenbaum E., Gourdin W.H., Hawley R.A., Honig J., House R.K., Jancaitis K.S., LaFortune K.N., Larson D.W., Le Galloudec B.J., Lindl J.D., MacGowan B.J., Marshall C.D., McCandless K.P., McCracken R.W., Montesanti R.C., Moses E.I., Nostrand M.C., Pryatel J.A., Roberts V.S., Rodriguez S.B., Rowe A.W., Sacks R.A., Salmon J.T., Shaw M.J., Sommer S., Stolz C.J., Tietbohl G.L., Widmayer C.C., Zacharias R., *Description of the NIF laser*, Fusion Science and Technology **69**(1), 2016: 25-145. https://doi.org/10.13182/FST15-144

[5] Zacharias R.A., Bliss E.S., Winters S., Sacks R.A., Feldman M., Grey A., Koch J.A., Stolz C.J., Toeppen J.S., Van Atta L., Woods B.W., *Wavefront control of high-power laser beams in the National Ignition Facility (NIF)*, Proceedings of the SPIE, Vol. 3889, Advanced High-Power Lasers, 2000. https://doi.org/10.1117/12.380902

[6] Shi F., Dai Y., Peng X., Song C., *Magnetorheological finishing for high-precision optical surface*, Optics and Precision Engineering **17**(8), 2009: 1859-1864.

[7] Wilkins P.R., Knight P.D., English R.E., *et al.*, *NIF optical specifications and means to quantify mounting stresses*, American Society for Precision Engineering, 1999: 1-4.

[8] Hui Wang, Zheng Zhang, Kai Long, Tianye Liu, Jun Li, Changchun Liu, Zhao Xiong, Xiaodong Yuan, *Back-support large laser mirror unit: Mounting modeling and analysis*, Optical Engineering **57**(1), 2018: 015109. https://doi.org/10.1117/1.OE.57.1.015109

[9] Wang Hui, Li Qin, Xiong Zhao, Yuan Xiaodong, Yao Chao, Rong Yiming, *Assembly error analysis for large aperture transport mirror in high power solid-state laser system*, Acta Optica Sinica, Issue 9, 2015: 262-269.

[10] Zhang Zheng, Quan Xusong, Wang Hui, Yao Chao, Rong Yiming, *Low-stress mounting configuration design for large aperture laser transmission mirror*, Acta Optica Sinica, Issue 1, 2017: 215-223.

[11] Li Guihua, Wang Hui, Xiong Zhao, Gao Liang, Cao Tingfen, Zhou Hai, *Surface error analysis of large reflecting mirror under assembly fastening forces*, China Mechanical Engineering **26**(9), 2015: 1173-1178.

[12] Noailles S., Bart T., Schmitz P., Hugget A., Ferbos R., Bouillet S., Leymarie C., Martin S., *Mechanical support system of laser megajoule large-dimension optical components*, Proceedings of the SPIE, Vol. 6665, New Developments in Optomechanics, 2007: 66650Z. https://doi.org/10.1117/12.731587

Received June 25, 2022